Sonochemical synthesis of nanocrystalline LaFeO$_3$

M. Sivakumar,[a] A. Gedanken,*[a] W. Zhong,[b] Y. H. Jiang,[b] Y. W. Du,[b] I. Brukental,[c] D. Bhattacharya,[c] Y. Yeshurun[c] and I. Nowik[d]

[a]Department of Chemistry, Bar-Ilan University, Ramat-Gan 52900, Israel.
 E-mail: gedanken@mail.biu.ac.il; Fax: 972-3-5351250; Tel: 972-3-5317769
[b]National Laboratory of Solid State Microstructures, Nanjing University, Nanjing
 210093, P. R. China
[c]Institute of Superconductivity, Department of Physics, Bar-Ilan University, Ramat-Gan
 52900, Israel
[d]The Racah Institute of Physics, The Hebrew University, Jerusalem 91904, Israel

Nanocrystalline perovskite-type LaFeO$_3$ with particle size of about 30 nm was prepared by a sonochemical method using iron pentacarbonyl and lanthanum carbonate as starting materials. The overall process involves three steps: formation of lanthanum carbonate using lanthanum nitrate and urea; reaction of the so-formed lanthanum carbonate with iron pentacarbonyl resulting in the formation of a precursor; calcination of the precursor to obtain nanocrystalline particles of LaFeO$_3$. Transmission electron microscopy revealed the particles to have a mean size of about 30 nm. Study of the magnetic properties of nanocrystalline LaFeO$_3$ particles shows a coercivity of ∼250 Oe, while the saturation magnetization is ∼40 memu g^{-1}.

Introduction

Research in submicroscopic or nanocrystalline materials continues to attract the interest of many scientists and engineers due to the large differences found in their properties when the particle size is reduced, and therefore possible new technological applications can arise. Lau et al.[1] have stated that nanocrystalline materials provide scientists and engineers a unique opportunity to obtain materials having properties that are otherwise unachievable with equilibrium materials. Conventional composite oxides such as LaFeO$_3$ and related compounds have been reported to be of importance due to their wide uses in fuel cells,[2] catalysts,[3,4] membranes in syngas production,[5] sensors,[6,7] and environmental monitoring applications.[8]

For the synthesis of LaFeO$_3$ and related compounds, methods involving solid state reaction,[9] hydrothermal synthesis,[10] combustion synthesis,[11,12] sol–gel,[13] precipitation[14] and reverse drop co-precipitation with poly(vinyl alcohol) as a protecting agent[15] have been reported in the literature. However, the conventional solid state reaction method requires several heating and grinding steps to ensure the homogeneous mixing of the various oxides,[16] while the reverse drop co-precipitation method[15] requires the use of more chemicals and longer time for the formation of the LaFeO$_3$. Also, all the wet chemical methods need a very high calcination temperature and a long soaking to obtain the desired final powders with good crystalline structure. Processes involving a higher calcination temperature and a longer soaking have several problems, e.g., poor homogeneity and high porosity of the samples, no control of the particle size, etc., which indirectly affects the functional properties of the obtained powders. Obtaining nanosized powders have therefore been difficult. To lower the preparation temperature and to obtain an ultrafine and chemically pure powder of LaFeO$_3$, much effort has been spent recently on the development of chemical methods. For this reason, it is of great significance to synthesise high quality LaFeO$_3$ powder. In view of these problems, this paper reports on the synthesis of LaFeO$_3$ using a novel sonochemical method involving the use of lanthanum carbonate and iron pentacarbonyl as reactants. The main advantage of this method is achieving good product formation, which is composed of fine particles of nanometric dimensions. The use of such a sonochemical method to synthesize LaFeO$_3$ has also been explored for the first time. The resulting material is of importance as it may have different electrical, magnetic and structural properties depending upon the method of preparation, starting materials and temperature.[17]

The present method makes use of ultrasound irradiation in two stages: (i) to synthesize uniform rods of La$_2$O-(CO$_3$)$_2$·1.4·H$_2$O, (ii) decomposing Fe(CO)$_5$ and dispersing the in situ formed amorphous Fe$_2$O$_3$ on the prepared La$_2$O-(CO$_3$)$_2$·1.4·H$_2$O obtained in the first stage, to obtain the precursor. Calcining this precursor then results in the formation of a fine LaFeO$_3$ powder.

Experimental

Materials

The starting materials used in the present work included lanthanum nitrate hexahydrate (Aldrich, 99.99%), urea (Aldrich, 98%), Fe(CO)$_5$ (Strem chemicals, USA, 99.5%), decalin, C$_{10}$H$_{18}$ (Acros organics, 98%) and pentane (96%, Bio-lab, Israel).

Characterisation

The phase constitution of the hexaferrite powder was recorded by employing a Rigaku X-ray diffractometer (Model-2028, Co-Kα). XRD measurements were taken in the 2θ scanning range from 15 to 70°. The microstructures of the products were determined by transmission electron microscopy (TEM) (JEOL-JEM 100SX microscope). Samples for TEM were prepared by placing a drop of the sample suspension on a copper grid coated with carbon (400 mesh, Electron Microscopy Sciences) and allowing it to dry in air. FTIR spectra were recorded on a Nicolet (Impact 410) infrared spectrophotometer with KBr pellets over the 400–3000 cm^{-1} range. Thermogravimetric analysis was performed in an oxygen atmosphere using a

Mettler Toledo TGA/SDTA851 instrument attached to a mass spectrometer (Balzers Instruments), over the temperature range of 30–900 °C (heating rate ~10 °C min^{-1}). Energy-dispersive analytical X-ray (EDAX) spectra were measured on a JEOL-JSM-840 scanning microscope. Mössbauer effect spectroscopy (MES) studies were performed using a ^{57}Co:Rh source (50mCi) and a conventional constant acceleration Mössbauer drive. Room-temperature magnetic properties were measured using a vibrating sample magnetometer (VSM).

Preparation procedures

Stage 1: preparation of La$_2$O(CO$_3$)$_2$·1.4·H$_2$O. The synthesis of lanthanum carbonate particles was carried out with the aid of ultrasound radiation and the process followed is similar to that as reported by Jeevanandam *et al.*[18] 120 ml of the experimental solution was irradiated for 3 h with high intensity ultrasound radiation by employing a direct immersion titanium horn (Sonics and Materials, 20 kHz, 600 W). Calorimetry was used to estimate the electro-acoustic or energy transfer efficiency of the transducer to the solution, in the present experiments. Based on the calorimetry experiments, the transfer efficiency of the ultrasonic energy from the transducer to the reactor solution was estimated as 54% (at 65% amplitude), with the assumption that all the ultrasonic energy was converted to heat in the reactor. Based on these calorimetry measurements, the power intensity of the system was calculated as 29.7 W cm^{-2}. The titanium horn tip was inserted into the solution to a depth of 1 cm. The temperature during the experiment increased to a maximum of 85 °C due to ultrasound passage, as measured by an iron–constantan thermocouple. After the precipitation process was complete, the precipitates were separated from the solution by centrifugation. The recovered precipitates were then washed several times with doubly distilled water and ethanol and then dried under vacuum at room temperature.

The role of urea in the homogeneous precipitation of lanthanum carbonate particles is that it decomposes by hydrolysis homogeneously in the solution upon heating, producing CO_3^{2-}, OH^- and NH_4^+ ions in solution. This increase in the pH of the medium is suitable for the formation of lanthanum carbonate particles. Measurement of the pH before and after the ultrasound irradiation treatment revealed that the pH of the solution increased from 5.6 to 6.4. Applying ultrasound radiation during the reaction might accelerate the homogeneous precipitation process. In addition to this, it might also be beneficial in controlling the particle size and the shape.

Stage 2: preparation of amorphous Fe$_2$O$_3$ from Fe(CO)$_5$ and *in situ* dispersion of the obtained product on La$_2$O(CO$_3$)$_2$·1.4·'''H$_2$O. This step utilizes the principle of obtaining pure amorphous materials from suitable precursors by means of sonication.[19,20] Suslick *et al.* have already prepared pure amorphous iron,[19] amorphous cobalt, amorphous Fe/Co alloy[21] and amorphous molybdenum carbide,[22] using ultrasound. Following the same principle, the present approach involves generating amorphous Fe$_2$O$_3$ from iron pentacarbonyl by ultrasound after which the resultant amorphous Fe$_2$O$_3$ was dispersed *in situ* on lanthanum carbonate, again with the assistance of ultrasound. The process involves taking stoichiometric amounts of La$_2$O(CO$_3$)$_2$·1.4·H$_2$O and Fe(CO)$_5$ in decalin and irradiating with ultrasound (the method followed is similar to stage 1). The reaction was carried out in an atmosphere of air at 0 °C for 4 h, after which the obtained product was thoroughly washed with pentane, centrifuged, and dried in vacuum at room temperature. The product thus obtained will hereafter be referred to as the precursor. This precursor was calcined at 800 °C for 24 h in air to obtain the lanthanum ferrite fine powder.
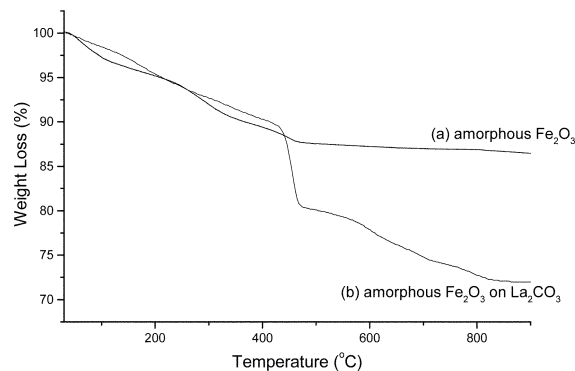
Fig. 1 TGA results of the as-synthesized amorphous Fe$_2$O$_3$ and precursor (amorphous Fe$_2$O$_3$ dispersed on La$_2$O(CO$_3$)$_2$·1.4·H$_2$O).

Results and discussion

(A) Thermal analysis by TGA

Fig. 1 shows the TG curves of amorphous iron oxide and amorphous iron oxide coated on lanthanum carbonate. Fig. 1(b) depicts the TG curve for the as-synthesized precursor in stage 2. This TGA shows weight loss in multiple steps from 30 °C up to 800 °C and the total weight loss is 27.3%. Thus, the excess weight loss in this case (8.4%), considering the theoretical carbonate decomposition weight loss (25.7%), should be confined to the weight loss stages of amorphous Fe$_2$O$_3$. For comparison, Fig. 1(a) shows the TGA curve for the sonochemical as-synthesized amorphous Fe$_2$O$_3$ obtained by decomposition of Fe(CO)$_5$ alone. In this curve, the weight loss starts from 30 °C and continues up to 475 °C. One possibility causing the weight loss in this stage might be desorption of unreacted iron carbonyl from the surface of the iron oxide. However, from the IR analysis (as described later on), the sample does not show any carbonyl peaks. Instead, it clearly shows peaks indicating the presence of oxalate ion and thus the weight loss can be ascribed to this ion. Also, it has already been found that by heating the amorphous Fe$_2$O$_3$, to around 300 °C, it loses its amorphous character and becomes crystalline.[20,23] The temperature of the final weight loss for the precursor is completed around 800 °C and the formation of LaFeO$_3$ is observed in the last plateau above 800 °C.

(B) XRD

From the literature we found that in order to obtain pure and well-crystallized LaFeO$_3$, it is necessary to subject the materials for calcination at 1000 °C for 184 h.[24] For shorter periods of time X-ray patterns still show peaks of La$_2$O$_3$ and α-Fe$_2$O$_3$ that have not reacted. However, in the present sonochemical method, it is observed that LaFeO$_3$ crystallises at temperatures as low as 800 °C. Fig. 2 shows the XRD pattern of LaFeO$_3$, amorphous Fe$_2$O$_3$ on La$_2$O(CO$_3$)$_2$·1.4·H$_2$O and amorphous Fe$_2$O$_3$. The pattern of LaFeO$_3$ is indexed as orthorhombic perovskite-type LaFeO$_3$ and shows a high degree of crystallinity.

Fig. 2(b) illustrates the XRD pattern of the precursor product obtained by sonicating a decalin solution of Fe(CO)$_5$ and La$_2$O(CO$_3$)$_2$·1.4·H$_2$O. The XRD pattern of this precursor is very similar to the pattern of lanthanum carbonate.[18] However, the colour of the product obtained in this case is black, whereas La$_2$O(CO$_3$)$_2$·1.4·H$_2$O obtained in stage 1 is white. This is due to the application of ultrasound on the Fe(CO)$_5$, which generates amorphous Fe$_2$O$_3$. The amorphous Fe$_2$O$_3$ was then dispersed or coated on La$_2$O(CO$_3$)$_2$·1.4·H$_2$O again with the assistance of ultrasound. In order to confirm this, a solution of Fe(CO)$_5$ in decalin alone was sonicated at 0 °C for 4 h and the colour of the product obtained is also black. Fig. 2(a) shows the XRD pattern of the
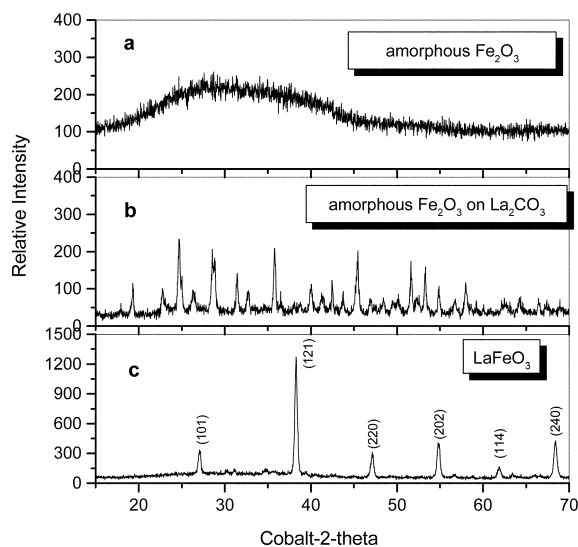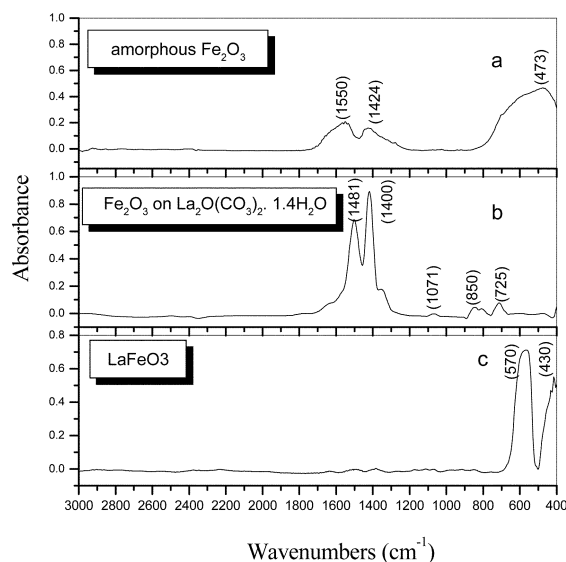
Fig. 2 Powder X-Ray diffraction patterns of (a) amorphous Fe$_2$O$_3$, (b) amorphous Fe$_2$O$_3$ dispersed on La$_2$O(CO$_3$)$_2$·1.4·H$_2$O and (c) LaFeO$_3$ obtained by calcining the precursor at 800 °C in air for 24 h.

Fig. 3 IR spectra of (a) amorphous Fe$_2$O$_3$, (b) amorphous Fe$_2$O$_3$ dispersed on La$_2$O(CO$_3$)$_2$·1.4H$_2$O and (c) LaFeO$_3$ obtained by calcining the precursor at 800 °C in air for 24 h.

resultant product obtained during this process. It can be seen from this pattern that the Fe$_2$O$_3$ obtained in this process is amorphous. The absence of this amorphous background due to Fe$_2$O$_3$ in Fig. 2(b) may be due to the dominance of crystalline La$_2$O(CO$_3$)$_2$·1.4·H$_2$O peaks. Fig. 2(c) shows the XRD pattern of LaFeO$_3$ obtained by calcining the precursor sample at 800 °C in air atmosphere for 24 h. The diffraction peaks match those reported for standard LaFeO$_3$ (JCPDS file No. 37-1493). Heating the precursor at a rate of 8 °C min^{-1} to 800 °C resulted in a well-crystallized ferrite phase. This was indicated by the appearance of the most intense reflections: (121), (202) and (240) peaks at 2θ values of 38.28, 54.78 and 68.43°, respectively, as shown in Fig. 2(c). Thus, the formation of LaFeO$_3$ is completed at 800 °C. The formation temperature for LaFeO$_3$ by the sonochemically prepared precursor is clearly lower than that observed in the conventional solid-state reaction utilizing La$_2$O(CO$_3$)$_2$·1.4·H$_2$O and Fe$_2$O$_3$ ($\sim$1000 °C for 184 h) for forming a single phase of LaFeO$_3$[24]. Thus, the formation temperature of LaFeO$_3$ by this process compares reasonably well with many other chemistry based processing routes.

(C) IR

The IR spectra of the amorphous iron oxide coated on lanthanum carbonate, amorphous iron oxide (for comparison) and calcined nanocrystalline LaFeO$_3$ powder in the wavenumber range from 3000 to 400 cm^{-1} are shown in Fig. 3(a)–(c). The IR spectrum of Fig. 3(b) provides evidence for the presence of carbonate ions of La$_2$O(CO$_3$)$_2$·1.4H$_2$O in the precursor; it also shows a broad band at *ca.* 1400 cm^{-1}, which is assigned to the bending vibrational mode of bound water molecules.[18] The absorption band at *ca.* 1481 cm^{-1} is attributed to the v_3 mode of the CO$_3^{2-}$ ion while the other bands at *ca.* 1071, 850 and 725 cm^{-1} have been assigned to the v_1, v_2 and v_4 modes of the carbonate ions, respectively.[18] The above observed bands clearly indicate the presence of carbonate ions in the precursor. However, this spectrum does not show the peaks for amorphous Fe$_2$O$_3$ which might be due to the relatively high intensity peaks of lanthanum carbonate. The IR spectrum of the amorphous Fe$_2$O$_3$ synthesized by ultrasound alone (for comparison) shows absorption bands at 473, 1424 and 1550 cm^{-1} (Fig. 3(a)). Also, the peaks observed at 1424 and 1550 cm^{-1} support the presence of oxalate ion. In addition, the peak centered at 473 cm^{-1} indicates the presence of amorphous iron oxide.[25] Fig. 3(c) shows the IR spectrum of LaFeO$_3$. This spectrum shows well-established strong absorption bands at $\sim$570 and $\sim$430 cm^{-1} in the powder calcined at

800 °C indicating the formation of lanthanum ferrite. The 570 cm^{-1} band is attributed to the Fe–O stretching vibration (v_1 mode), and the 430 cm^{-1} band corresponds to the O–Fe–O deformation vibration (v_2 mode).[26] Comparing, Fig. 3(c) with Fig. 3(a) and (b), we can see after calcination that the characteristic bands of La$_2$O-(CO$_3$)$_2$·1.4H$_2$O and iron oxide vanish at this calcination temperature and only Fe–O stretching vibration bands are found in the synthesised powder. The above interpretation of the IR spectral results is based on the assumption that the synthesized carbonate, Fe$_2$O$_3$, precursor, and lanthanum ferrite are essentially pure materials. These results agree with the XRD phase-analysis findings.

(D) EDAX

Elemental analysis using EDAX indicates that the product of calcination obtained from the precursor has a La:Fe ratio of 1:1 (within the range 0.98–1.01) indicating the equal presence of La and Fe in the sample. Also, a similar analysis for the amorphous Fe$_2$O$_3$ obtained from Fe(CO)$_5$ shows the presence of Fe and O in a ratio ranging from 1:1.5 to 1:2. The higher ratio is due to the strong adsorption of oxygen as has been reported by Cao *et al.*[23] No other elements were detected in the EDAX of the amorphous compound.

(E) Mössbauer studies

As confirmation of the phase purity of the prepared samples, Fig. 4 shows the ^{57}Fe Mössbauer spectrum measured at 27 °C
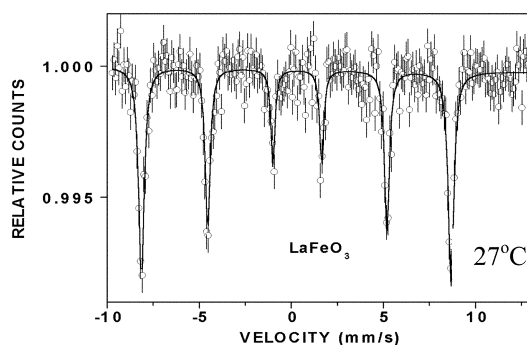
**Fig. 4** Mössbauer spectrum of the LaFeO$_3$ sample obtained by calcining the precursor at 800 °C in air for 24 h.

of the LaFeO$_3$ powder calcined at 800 °C for 24 h in air. A theoretical spectrum (the solid line) least-squared fitted to the experimental points, yields the following hyperfine interaction parameters: isomer shift relative to iron metal: 0.30(3) mm^{-1}, Quadrupole interaction $Q/2 = -0.06(3)$ mm^{-1}, and magnetic hyperfine field 521(2) kOe. These parameters agree perfectly with those of bulk LaFeO$_3$.[27]

(F) Permeability spectra

A useful route to investigate the mechanism of domain wall motions and domain rotations is to measure the complex permeability ($\mu^* = \mu' - i\mu''$) as a function of frequency, i.e., the so-called magnetic spectrum. In addition, by studying such a magnetic spectrum, the effective magnetic anisotropy field, as well as the damping mechanism of domain wall displacements, can be checked. In general, the dispersions caused by wall displacements occur in a radio frequency range (below 10 MHz), and those caused by domain rotations often appear in the microwave range (100 MHz to 10 GHz). This methodology has been extensively used in ferrites.[28,29] Thus, a similar study has been carried out for the LaFeO$_3$ powder prepared by the present ultrasonic method and calcination at 800 °C for 24 h in air.

The frequency dependence of the complex permeability (real part μ' and imaginary part μ'') is shown in Fig. 5. For permeability measurements, the nanosized powder sample was pressed to a ring with a typical size of 13 mm OD, 7 mm ID and 1 mm thickness. The pressed ring has a lower density than the sintered one. For polycrystalline ferrites, the permeability is related to the magnetizing mechanisms: spin ratation and domain wall motion. According to theory, in single domain grains there are no domain wall motions. Therefore, μ_0 (static permeability, i.e. μ' with frequency limit to zero) is only caused by reversible domain rotations and follows the relation $\mu_0 = 1 + 8\pi M_s/3H_a$, where H_a is the effective magnetic anisotropy field. Because M_s of LaFeO$_3$ is very small, the complex permeability is small. In addition, the nonmagnetic impurities such as boundaries and cavities from the low-density sample may cause the permeability to decline further. In the corresponding bulk sample, there is domain wall motion, whereas, in nanosized samples, there are only reversible domain rotations. The μ_0 contributed by domain rotations is generally smaller than that by domain wall displacements. It shoud be noted that the imaginary part μ'' of nanocrystalline perovskite-type LaFeO$_3$ is very small, which may be important for further nanocrystalline dielectric materials development.
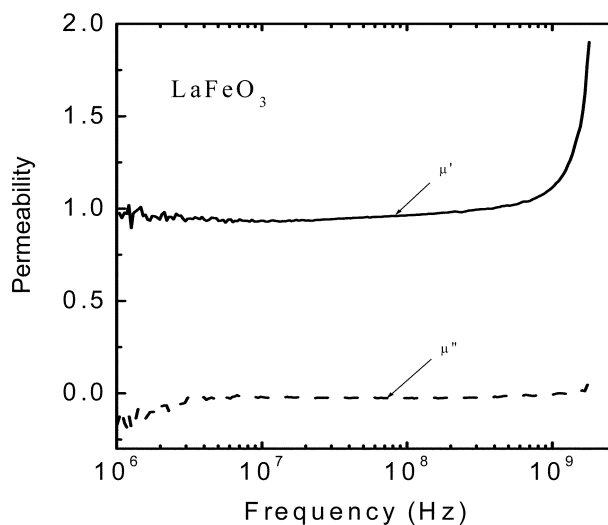
Fig. 5 Plots of complex permeability as a function of frequency for a polycrystalline LaFeO$_3$ sample at room temperature.
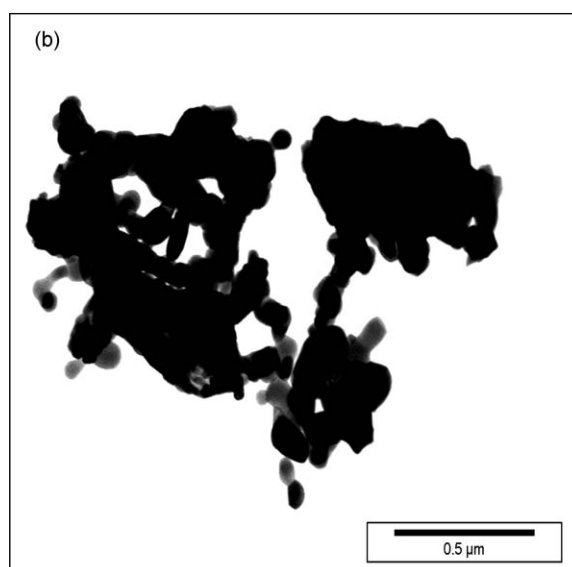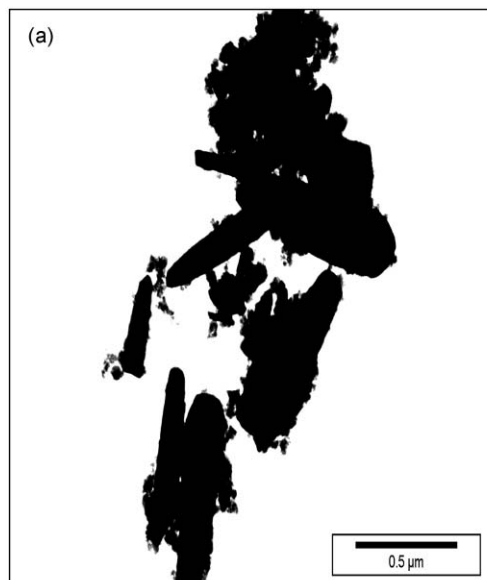
Fig. 6 (a) Transmission electron micrograph of amorphous Fe$_2$O$_3$ dispersed on La$_2$O(CO$_3$)$_2$·1.4H$_2$O and (b) transmission electron micrograph of LaFeO$_3$ obtained by calcining the precursor at 800 °C in air for 24 h.

(G) TEM

Fig. 6(a) depicts a TEM image of the amorphous Fe$_2$O$_3$ powder dispersed on the hexagonal La$_2$O(CO$_3$)$_2$·1.4H$_2$O rods (average diameter and length are 1.0 and 0.15 μm, respectively).

It is clearly seen that there is no crystalline formation of Fe$_2$O$_3$ in this powder. It can also be observed that this amorphous Fe$_2$O$_3$ is an agglomerate of small particles aggregated in a spongelike form. The micrograph in Fig. 6(b) indicates the morphology of the lanthanum ferrite sample obtained after treating the precursor at 800 °C. It can be observed from this micrograph that after calcination, the particles have an average diameter of about 30 nm, which further confirms the nanometer dimensions of the particles. No remaining La$_2$O(CO$_3$)$_2$·1.4H$_2$O and Fe$_2$O$_3$ could be observed in the micrograph in spite of the low heating treatment temperature. This result agrees with the results of XRD and IR.

(H) Magnetic properties of nanocrystalline LaFeO$_3$

Fig. 7 shows a magnetic hysteresis loop of nanocrystalline LaFeO$_3$ obtained by the present sonochemical method. We have measured the magnetic properties of the nanocrystalline
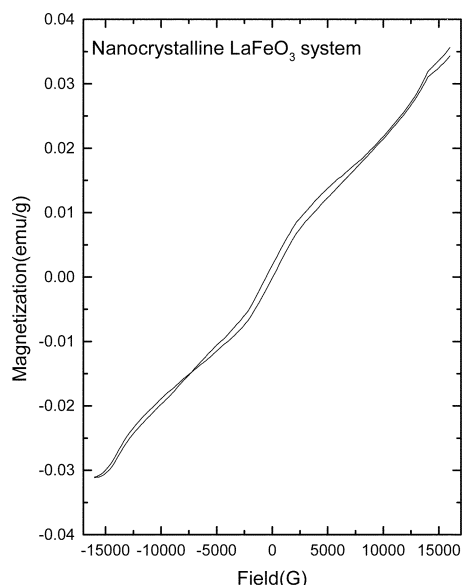
Fig. 7 The magnetization *vs.* applied field (measured at room temperature) pattern for the ultrafine LaFeO$_3$ system prepared by a sonochemical technique followed by calcination at 800 °C in air for 24 h.

LaFeO$_3$ at room temperature using a vibrating sample magnetometer (VSM). From the hysteresis plot, we can observe hysteresis but no clear saturation of magnetization within the field limit of ~16000 Oe. Normally, the LaFeO$_3$ system is either weakly ferromagnetic (WFM) or antiferromagnetic (AFM) with a Néel temperature T_N ~ 477 °C.[30] For a 30 nm LaFeO$_3$ particle size system, Qi *et al.*[31] reported a coercive field of ~90 G and a saturation magnetization M_s of ~2.75 emu g^{-1} at room temperature. In our case, the corresponding values are ~250 Oe and ~40 memu g^{-1}, respectively. This reflects a further increase in the magnetocrystalline anisotropy, which is expected in the nanocrystalline system. The squareness ratio M_r/M_s in our case is ~0.055, which is quite small, compared to the value (~0.135) reported.[31] All these results point out to the presence of a large number of fine particles in our system. The average particle size of our system is ~30 nm.

In the conventional solid-state reaction of Fe$_2$O$_3$ with lanthanum carbonate to form the lanthanum ferrite, the major limitation is the diffusion factor. In the present sonochemical method this diffusion resistance may be overcome, as there is an *in situ* generation of amorphous Fe$_2$O$_3$ from Fe(CO)$_5$ by ultrasound, followed by its dispersion or deposition on lanthanum carbonate, again assisted by ultrasound. This process might facilitate the diffusion, as well as the reaction, of highly reactive lanthanum ion (La^{3+}) with the amorphous Fe$_2$O$_3$, resulting in the completion of the phase transition of the precursor to the LaFeO$_3$ ferrite at a lower calcination temperature of 800 °C, employed in the present method.

The amorphous nature of Fe$_2$O$_3$ synthesized by ultrasound might also play a key role in increasing its reactivity with lanthanum carbonate, resulting in the formation of a ferrite phase at the lower calcination temperature. The importance of amorphicity in increasing the reactivity has already been discussed.[32] Bellisent *et al.*[21] have clearly shown that sonochemically prepared amorphous Fe, Co and Fe–CO nanomaterials are better catalysts than the corresponding crystalline nanomaterials prepared by other methods. In addition, Yee *et al.*[33] have functionalized amorphous Fe$_2$O$_3$ nanoparticles with alkanesulfonic and octadecanephosphonic acids. This work further supports the fact that it is possible to form a coating of organic molecules more easily on amorphous Fe$_2$O$_3$. In addition to the above factors, the size of the reactants

(specifically, amorphous Fe$_2$O$_3$) also contributes to the lowering of calcination temperature. It can be seen from the work of Vazquez-Vazquez *et al.*[24] that by using conventional lanthanum and iron nitrates, the mean particle size of the ferrite obtained is about 120 nm, at a calcination temperature of 800 °C. In addition, formation of the secondary phases of La(OH)$_3$, α-Fe$_2$O$_3$ and ferrihydrite have also been noted at this temperature. It has also been found that a temperature of 1000 °C for 184 h is necessary to obtain pure and well-crystallized LaFeO$_3$. However, in the present case, by applying a calcination temperature of 800 °C for 24 h, the mean particle size of the obtained ferrite is 30 nm and no secondary phases are observed, which might be due to the highly reactive amorphous Fe$_2$O$_3$ generated by ultrasound already present in the system.

Conclusions

In the present investigation, LaFeO$_3$ has been synthesized from lanthanum carbonate and iron pentacarbonyl *via* a sonochemical method for the first time. The sonochemically synthesized LaFeO$_3$ is a nanocrystalline material with high purity and good homogeneity. It was obtained with lower processing temperatures and shorter annealing times. The obtained nanoferrite powder is expected to be used in applications for functional ceramics (sensors, SOFCs, electrodes, or even magnetic and ferroelectric applications).

Acknowledgements

References

1   M. L. Lau, H. G. Jiang, R. J. Perez, J. Juarezislas and E. J. Lavernia, *Nanostruct. Mater.*, 1996, **7**, 847.
2   N. Q. Minh, *J. Am. Ceram. Soc.*, 1993, **76**, 563.
3   A. Delmastro, D. Mazza, S. Ronchetti, M. Vallino, R. Spinicci, P. Brovetto and M. Salis, *Mater. Sci. Eng. B*, 2001, **79**, 140.
4   S. L. Bai, X. X. Fu, J. Z. Wang, Q. H. Yang, Y. H. Sun and S. L. Zeng, *Chin. J. Appl. Chem.*, 2000, **17**, 343.
5   Q. Ming, M. D. Nersesyan, A. Wagner, J. Ritchie, J. T. Richardson, D. Luss, A. J. Jacobson and Y. L. Yang, *Solid State Ionics*, 1999, **122**, 113.
6   T. Arakawa, H. Kurachi and J. Shiokawa, *J. Mater. Sci.*, 1985, **20**, 1207.
7   Y. Shimizu, M. Shimabukuro, H. Arai and T. Seiyama, *Chem. Lett.*, 1985, **163**, 917.
8   G. Martinelli, M. C. Carotta, M. Ferroni, Y. Sadaoka and E. Traversa, *Sens. Actuators B*, 1999, **55**, 99.
9   B. I. Ita, Ph.D Thesis, University of Calabar, Nigeria, 1998.
10 W. J. Zheng, R. H. Liu, D. K. Peng and G. Y. Meng, *Mater. Lett.*, 2000, **43**, 19.
11 S. S. Manoharan and K. C. Patil, *J. Solid State Chem.*, 1993, **102**, 267.
12 A. Chakraborty, P. S. Devi and H. S. Maiti, *J. Mater. Res.*, 1995, **10**, 918.
13 J. Xiao, G. Y. Hong, D. C. Yu, X. T. Dong, D. J. Wang, L. Jiang and T. J. Li, *Acta Chim. Sin.*, 1994, **52**, 784.
14 N. Pandya, R. G. Kulkarni and P. H. Parsania, *Mater. Res. Bull.*, 1990, **25**, 1073.
15 X. Li, H. B. Zhang and M. Y. Zhao, *Mater. Chem. Phys.*, 1994, **37**, 132.
16 P. Ravindranathan, S. Komarneni and R. Roy, *J. Mater. Sci. Lett.*, 1993, **12**, 369.
17 B. I. Ita, U. J. Ekpe and U. J. Ibok, *Global J. Pure Appl. Chem.*, in press.
18 P. Jeevanandam, Y. Koltypin, O. Palchik and A. Gedanken, *J. Mater. Chem.*, 2001, **11**, 869.
19 K. S. Suslick, S. B. Choe, A. A. Cichowlas and M. W. Grinstaff, *Nature*, 1991, **353**, 414.

20 X. Cao, Y. Koltypin, R. Prozorov, G. Kataby and A. Gedanken, *J. Mater. Chem.*, 1997, **7**, 2447.

21 R. Bellissent, G. Galli, T. Hyeon, S. Magazu, D. Majolino, P. Migliardo and K. S. Suslick, *Phys. Scr.*, 1995, **T57**, 79.

22 T. H. Hyeon, M. M. Fang and K. S. Suslick, *J. Am. Chem. Soc.*, 1996, **118**, 5492.

23 X. Cao, R. Prozorov, Y. Koltypin, G. Kataby and A. Gedanken, *J. Mater. Res.*, 1997, **12**, 402.

24 C. Vazquez-Vazquez, P. Kogerler, M. A. Lopez-Quintela, R. D. Sanchez and J. Rivas, *J. Mater. Res.*, 1998, **13**, 451.

25 B. Grzeta, M. Ristic, I. Nowik and S. Music, *J. Alloys Compd.*, 2002, **344**, 304.

26 G. V. S. Rao, C. N. R. Rao and J. R. Ferraro, *Appl. Spectrosc.*, 1970, **24**, 436.

27 M. Eibschut, S. Shtrikma and D. Treves, *Phys. Rev.*, 1967, **156**, 562.

28 G. T. Rado, R. W. Wright and W. H. Emerson, *Phys. Rev.*, 1950, **80**, 273.

29 G. T. Rado, R. W. Wright, W. H. Emerson and A. Terris, *Phys. Rev.*, 1952, **88**, 909.

30 Y. N. Venevtsev and V. V. Gagulin, *Ferroelectrics*, 1994, **162**, 23.

31 X. W. Qi, J. Zhou, Z. X. Yue, Z. L. Gui and L. T. Li, *Mater. Chem. Phys.*, 2003, **78**, 25.

32 K. S. Suslick, T. W. Hyeon and M. M. Fang, *Chem. Mater.*, 1996, **8**, 2172.

33 C. Yee, G. Kataby, A. Ulman, T. Prozorov, H. White, A. King, M. Rafailovich, J. Sokolov and A. Gedanken, *Langmuir*, 1999, **15**, 7111.